

# PARAMETERS AND BEHAVIOUR OF NiCrFeSiB LASER CLADDING IN OVERLAPPED GEOMETRY

AI. PASCU<sup>1</sup>   E.M. STANCIU<sup>1</sup>   I.C. ROATĂ<sup>1</sup>  
C. CROITORU<sup>1</sup>   L.S. BALTEŞ<sup>1</sup>   M.H. TIHEREAN<sup>1</sup>

**Abstract:** *This paper addresses to the laser cladding of Ni17Cr4Fe 4Si3.5B1C powder in overlapped tracks geometry. Different process parameters like laser power, cladding speed and powder feed rate are designed in order to obtain defect free deposition and for enhance the hardness of the cladded layers. In transversal sections, the microstructure aspects of the cladded layers reveal the geometry and orientation of the dendrites, with different crystal morphology and size, depending on the used parameters. The study demonstrates that laser cladding is a complex process which is directly influenced by technological parameters. The Taguchi design of experiments reveal that powder feed rate has the most influence on the laser cladded layer geometry and mechanical proprieties.*

**Key words:** *laser cladding, Ni powder, cracking susceptibility.*

## 1. Introduction

Nowadays, the laser cladding is a usual technique for enhancement or reconditioning of metallic surfaces. Advantages such as precision, low dilution, good adhesion between clad - substrate and small heat affected zone are the key specifications which make the laser cladding a cost-effective industrial surfacing technique [6]. To date, many studies were made for single or multipass laser cladding process optimisation [15]. The necessity of performing metallic coatings on large surfaces, impose a high attention about laser cladding in partially overlapped tracks. It is well known that compared to single track cladding, the overlapped tracks have a high susceptibility

to hot cracking due to the high thermal gradients and cooling rates. This disadvantage may be combated by manipulation of the powder chemical composition. Nickel and cobalt base powders are widely used for coaxial laser cladding in many different market segments and applications. The Ni base powders have a high resistance to impact, to corrosive environments and generally good behaviour to high temperature. There are numerous investigations in which researchers try to obtain zero dilution and cracks free laser cladded layers of NiCrFe and NiCrFe + carbides/ceramics [3], [4].

According to Zhang et al. [14], the microhardness and wear resistance may be improved by mixing 1-3% nano size CeO<sub>2</sub> to NiCrFe powder. Another method to

---

<sup>1</sup> Dept. of Materials Engineering and Welding, *Transilvania University of Braşov*.

improve the hardness of Ni base powders is the addition of WC. NiCrBSi/WC-Ni composite clads on stainless steel substrate have been obtained by Guo et al. [2] as a method to enhance the tribological behaviour of coatings. Addition of 70% Ni into 30% WC-NiCrBSi improves the wear resistance of the coating according to Luo [7]. Wang [13] sustain that addition of  $V_2O_5$  enhance the toughness, refine the microstructure and reduce the cracking sensitivity of the high Ni alloy coating.

High hardness and wear resistance are obtained by using Ni-Cr-Fe-Si-B powders. In this case a major problem is represented by the hot cracking susceptibility due to chromium carbides and borides formation.

The process parameters optimisation is the solution to reduce this down-back [8]. Song et al. [11] reveals that the process parameters optimisation and Ni-Cr-Fe-Si-B composition adjustment is a good method to improve the forming microstructure, plasticity and toughness of the clad layer. According to Wang et al. [12] the cracking susceptibility increases with the area and thickness of the coating layer. It was also determined that majority of cracks are formed in the fusion zone and are perpendiculars to laser scanning direction. The crack formation during overlapped tracks and overlapped multilayer claddings is a major problem due to the continuously changing of the thermal gradient during the laser processing. J.M. Dowden [1] sustain that cracks are produced mainly due to residual stress induced in the clad layer. He concludes that cracks

are generated by the thermal contraction during the cooling process and by the different contraction factor between the coating and the substrate. As demonstrated [5] cracks can be suppressed by induction preheating, but with the disadvantages of a high dilution.

Our previous works define the optimal parameter window for single track laser cladding of Metco 15E powder [9], [10].

The present study tries to determine the optimal process parameter in terms of cracking susceptibility, hardness behaviour and geometry profile for multipass laser cladding and the solar heat treatment effect on the Inconel layer.

## 2. Experimental Procedure

### 2.1. Materials

The substrate used to perform the experimental cladding tests is low alloyed steel, namely AISI 5140. This grade of steel is used for components in automotive industry, where hardness and wear resistance of surface is necessary. The metal is normalised after moulding and the laser cladding processing on this substrate are used to improve the wear resistance or to recondition worn pieces.

The chemical composition of the base material is presented in Table 1 (analysed by SPECTROMAXx M spectrometer).

The Ni base powder, Metco 15 E, fabricated by Sulzer Metco USA was used as cladding material.

The chemical composition of the powder is presented in Table 2.

*Chemical composition of the base material*

Table 1

Material	Element wt. (%)									
	C	Cr	Si	Ni	Fe	Mn	S	Mo	P	Cu
AISI 5140	0.364	0.98	0.223	0.096	97.5	0.65	0.021	0.019	0.013	0.13
	Al	Co	Ti	N	Sb	Sn	V	W	Pb	
	0.026	0.0066	0.0006	0.017	97.5	0.0080	<0.0039	<0.0070	<0.0020	

*Chemical composition of Ni based powder*

Table 2

Power type	Chemical Element (%)						Powder average dimension 5-100 $\mu\text{m}$
	Ni	Cr	Fe	Si	B	C	
Metco15 E	Bal.	17	4	4	3.5	1	

The base material illustrated in Figure 1a and b has a ferrite-pearlite structure with lamellar pearlite.

Powder morphology is very important in the cladding process, due to the inherent problems related to the accumulation or wear of the cladding system components. For the experiments, powder with spherical shape has been used, emphasized by images of scanning electron microscopy (Figure 1b). The average powder dimension is comprised between 5  $\mu\text{m}$  and 110  $\mu\text{m}$ .

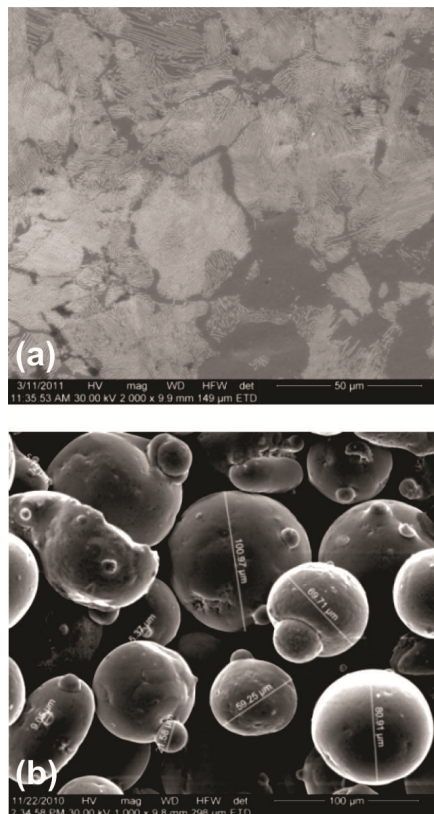


Fig. 1. *Optical and SEM micrograph of AISI 5140 base material and NiCrFeSiBC powder [10]*

## 2.2. Laser Cladding

The cladding tests were performed by direct coaxial injection using a Rofin YC3300 (1064 nm wavelength, 3.3 kW) laser. The powder injection was achieved by a Rofin type coaxial injection unit model Coax 8 manipulated by an ABB IRB 4400 robot and the powder was provided in the injection unit using SulzerMetco Single 10C equipment. Schematic representation of the laser cladding procedure is presented in the Figure 2.

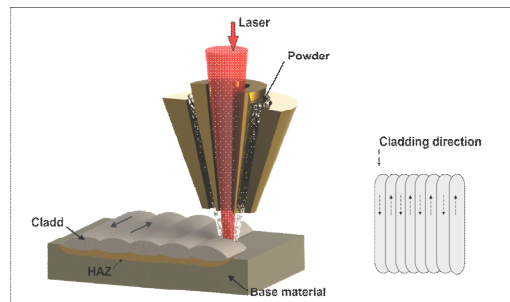


Fig. 2. *Experimental set-up used for the laser cladding tests*

The cladding layers were made on AISI 5140 steel samples with the size of 22x12x110 mm, that were previously grinded at 0.8  $\mu\text{m}$  roughness. To avoid the appearing of possible structural or chemical inhomogeneities, all the samples were made from the same material block. Depending on the designed overlapping degree, 10 to 12 overlapped layers of 70 mm length were cladded on each sample. A defocused 2.5 mm laser beam was used in order to obtain a low as possible dilution with the substrate.

### 3. Results and Discussions

The previous study [10] defined the values of the optimal parameters for a single track, during the laser cladding.

In this research the design of experiments method was used in order to decrease the number of experiments necessary for determining the optimal parameter for laser cladding with high Ni alloyed powder. The Taguchi DOF was used in order to determine which parameter has the most influence on the clad geometry and hardness. A three level design with two factors, namely clad high and hardness was employed for determination. In Tables 3 and 4 are presented the values of response for signal to noise and for means (correlated with Figure 3).

Table 3

*Response for signal to noise ratios,  
larger is better*

Level	Powder feed rate	Power	Speed
1	56.11	57.18	57.87
2	57.04	56.55	56.37
3	58.09	57.52	57.01
Delta	1.98	0.97	1.50
Rank	1	3	2

Table 4

*Response for means*

Level	Powder feed rate	Power	Speed
1	873.3	1268.0	1400.5
2	1109.5	1116.5	1061.7
3	1683.7	1282.0	1204.3
Delta	810.3	165.5	338.8
Rank	1	3	2

Table 5 presents the input laser cladding parameters variable and the response factors. Correlating with the Figure 3 it is clear that a major influence on the clad layer geometry is induced by the amount of powder and by the processing speed. The powder feed rate slope has a high influence on the clad high and hardness

mainly in the 10 to 13 g/min interval. The same slope appearance can be observed in the case of cladding speed in the interval between 14 to 18 mm/s. Therefore, the laser power has no significant effect in the laser cladding process compared with the powder amount and the scanning speed.

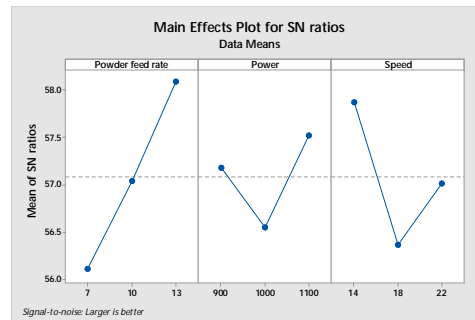
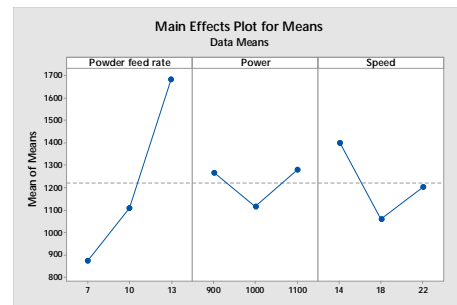


Fig. 3. Taguchi design of experiments response table for signal to noise ratio and means

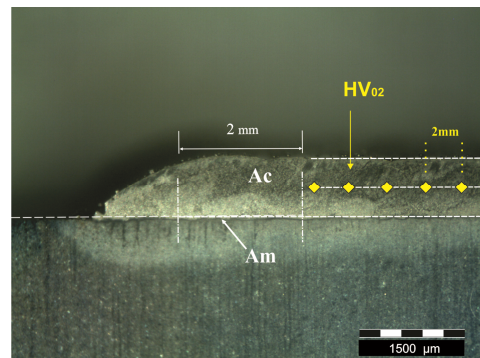


Fig. 4. Schematic representation of distribution of the microhardness testing and the geometric dilution determination  
Ac - clad area, Am - molten area



Table 5

*Test results (spot diameter 2.5 mm; 12 tracks; 1.2 mm overlap; 40 mm length)*

Crt.	Parameter s	Powder Feed Rate	Laser Power	Cladding Speed	Height	HV	Observation
	Code	F	P	S			
	Unit	[g/min]	[W]	[mm/s]			
1	Test 1.1	7	900	14	1484	509	superficial cracks
2	Test 1.2	7	1100	18	1109	461	No superficial cracks
3	Test 1.3	7	1300	22	1190	487	superficial cracks
4	Test 2.1	10	900	18	1362	474	superficial cracks
5	Test 2.2	10	1100	22	1288	482	superficial cracks
6	Test 2.3	10	1300	14	2398	653	No superficial cracks
7	Test 3.1	13	900	22	3148	631	superficial cracks
8	Test 3.2	13	1100	14	2789	570	superficial cracks
9	Test 3.3	13	1300	18	2422	542	superficial cracks

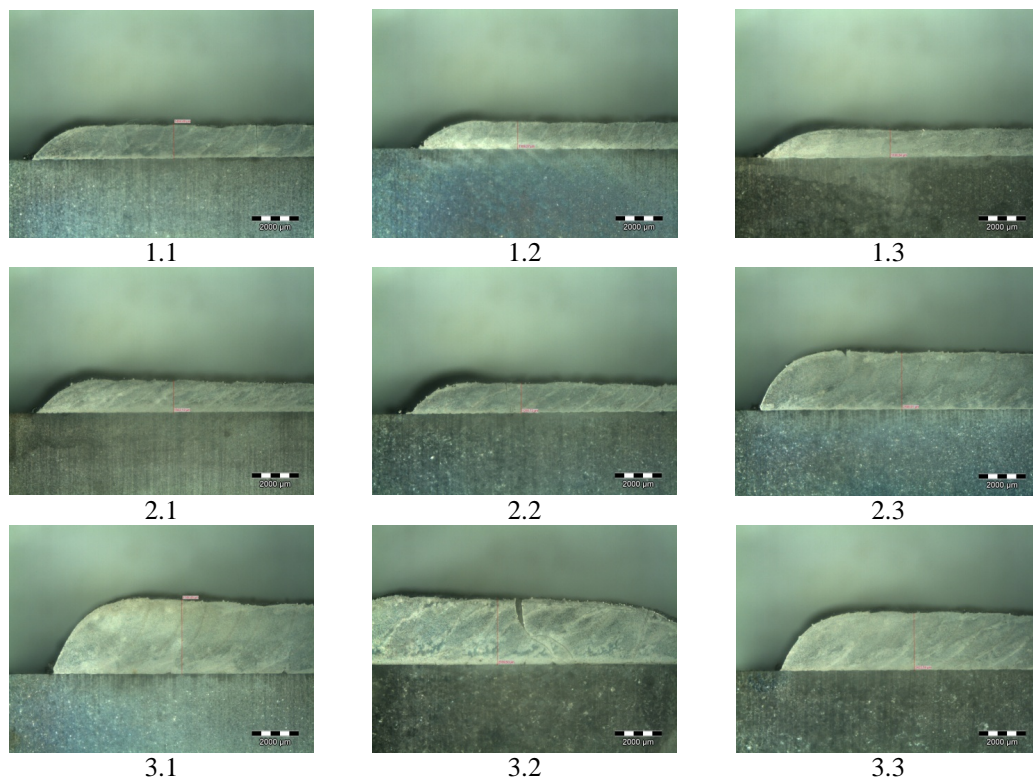


Fig. 5. Geometry profile of the laser cladded cross-sections

However, it is not enough to correlate the speed and powder feed rate in order to obtain a high quality cladded layer.

In the Table 5 is specified if the tests sample have or not superficial cracks occurred during the solidification process.

Even if all the samples present a very good geometry appearance only the samples 1.2 and 2.3 are superficial crack free. These samples were realised with medium value of powder feed rate and cladding speed. In case of sample 2.3 the higher laser power used is absorbed by the higher amount of powder promoting a better thermal distribution and deposition rate that minimize the dilution effect resulting in a higher microhardness. Microhardness analyses were performed using a Shimadzu HMV 2T microhardness tester. Five  $HV_{0.02}$  tests were made on each specimen (Figure 4) and the determined microhardness represents the average values of the five indentations.

The Figure 5 highlights the geometry of the partially overlapped cladded layers. The samples were prepared by cutting, grinding and polishing followed by a chemical etching in 2%  $HNO_3$  reagent. The macroscopic pictures from Figure 5 were realised using an Olympus SZX7 low magnification (5.6X) microscope. All layers show a very good bonding with the substrate with a minimum dilution. The calculated geometrical dilution (Eq. 1) is in the range of 2 to 4.5% which means that a high purity coated layer was deposited without mixture with the substrate.

$$\text{Dilution} = A_m / (A_c + A_m) \times 100 \quad (1)$$

The microstructure of the obtained coating is presented in the Figure 6. The base material presents a compact and quite uniform microstructure, with ferrite and specific lamellar pearlite grains (Figure 6d). Due to the relatively high carbon content in this steel, after the heat treatment or remelting process, the phase transformation area is susceptible to hardening, during fast cooling, promoting the formation of martensite.

During the cladding process this type of structure can develop the emergence of martensite in the heat affected zone (Figure

6e) with the drawback of high brittleness and hardness. Increasing of the microhardness was measured in this area from 235  $HV_{0.02}$  characteristic of the base material up to 485  $HV_{0.02}$ .

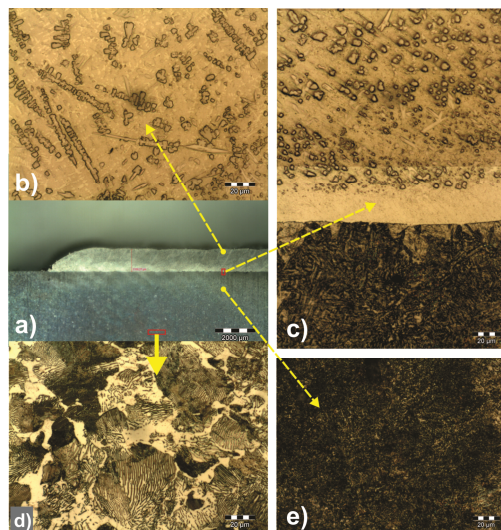


Fig. 6. Microstructure of the cladded layer and base material of sample 1.2

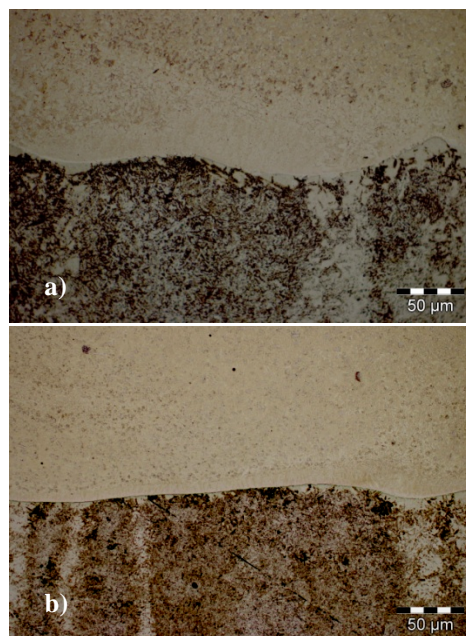


Fig. 7. Microstructure of the boundary zone between the cladded layer and the base material

At the boundary between the coating and the base material is a non-interference zone where the microstructure is formed mainly from dendrite structures enclosed in a high content nickel matrix. A detail of the boundary area is presented in the Figure 7a and b. It is obvious that strong bonding and low dilution was accomplished. It is a very good results considering that an usual dilution in case of laser cladding is around 25-30%. This good result was obtained due to the defocused laser beam that allows a better distribution of the thermal gradient at the surface of the substrate.

The Figure 8 describes the main types of microstructure of the laser and NiCrFeSiB alloy claddings.

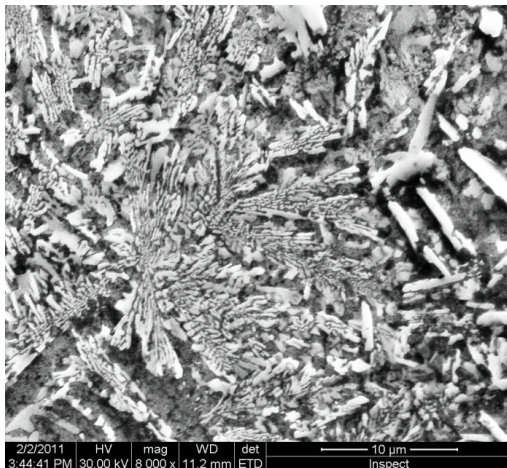


Fig. 8. *The SEM image of the cladded layer (section of sample 1.2)*

The dendrite structures developed in iron rich matrix can be found nearby the diffusion zone and are characterised by high percentage of iron diffused from the base material; the minimum hardness of the cladded layer is obtained in this zone. The superior mechanical properties of the NiCrFeSiB alloy are obtained in the upper part of the coated layer where the presence of complex carbides and borides dispersed in a nickel - iron matrix is observed (Figure 7).

The cracking susceptibility of the cladded layer is influenced by the distribution of the thermal gradient.

The samples realised with a higher power have more superficial cracks as can be seen in the macroscopic images from Figure 4. The samples processed at 1300 W have cracks initiated from the surface of the substrate up to the upper part of the cladded layer. The worse combined parameters are high laser power with low scanning speed because induce a high thermal gradient into the base material (example sample 3.2).

#### 4. Conclusions

The study presents a modern method for determining optimal parameters of the cladding process and the parameters that have higher influence on the geometry and mechanical proprieties of the cladded layer. By using 9 array Taguchi matrix it was determined that powder feed rate and cladding speed have a major influence on the laser cladding process.

The cracking behaviour of the samples shows that only in a narrow parameters window the cracks free layers can be obtained.

In the studied case is recommended that a laser power around 1000 W combined with a medium speed of 14 mm/s and a low amount of powder to be used.

Further investigations will be made on the influence of the overlapping degree on the geometry and mechanical proprieties of the multipass laser claddings.

#### References

1. Dowden, J.M.: *The Theory of Laser Materials Processing: Heat and Mass Transfer in Modern Technology*. Springer Science & Business Media Publishing House, 2009.
2. Guo, C., Chen, J., Zhou, J., Zhao, J., Wang, I., Yu, Y., Zhou, H.: *Effects of*



- WC-Ni Content on Microstructure and Wear Resistance of Laser Cladding, Ni-Based Alloys Coating*. In: *Surface & Coatings Technology* **206** (2012), p. 2064-2071.
3. Hemmati, I., Ocelík, V., De Hosson, J.Th.M.: *Effects of the Alloy Composition On Phase Constitution and Properties of Laser Deposited Ni-Cr-B-Si Coatings*. In: *Physics Procedia* **41** (2013), p. 302-311.
  4. Hemmati, I., Ocelík, V., De Hosson, J.Th.M.: *Laser Surface Engineering Processes and Applications*. A volume in Woodhead Publishing Series in Electronic and Optical Materials, 2015, p. 137-162.
  5. Huang, Y., Zeng, X.: *Investigation on Cracking behavior of Ni-Based Coating by Laser-Induction Hybrid Cladding*. In: *Applied Surface Science* **256** (2010) Issue 20, p. 5985-5992.
  6. John, C.I.: *Laser Processing of Engineering Materials*. Elsevier Butterworth-Heinemann, 2005.
  7. Luo, X., Li, J., Li, G.J.: *Effect of NiCrBSi Content on Microstructural Evolution, Cracking Susceptibility and Wear behaviors of Laser Cladding WC/Ni-NiCrBSi Composite Coatings*. In: *Journal of Alloys and Compounds* Volume **626** (2015), p. 102-111.
  8. Nenadl, O., Ocelík, V., Palavra, A., DeHosson, J.Th.M.: *The Prediction of Coating Geometry from Main Processing Parameters in Laser Cladding*. In: *Physics Procedia* **56** (2014), p. 220-227.
  9. Pascu, A., Hulka, I., Tierean, M.H., Croitoru, C., Stanciu, E.M., Roată, I.C.: *A Comparison of Flame Coating and Laser Cladding Using Ni Based Powders*. In: *Solid State Phenomena* **254** (2016), p. 77-82.
  10. Pascu, A.: *Parameters of the Laser Cladding Process*. Braşov. Lux Libris Publishing House. 2015.
  11. Song, J., Li, Y., Fu, J., Deng, Q., Hu, D.: *Cracking behavior of Laser Cladding Forming Nickel Based Alloys*. In: *Technology and Innovation Conference 2009 (ITIC 2009)*, 2009.
  12. Wang, F., Mao, H., Zhang, D., Zhao, X., Shen, Y.: *Online Study of Cracks during Laser Cladding Process Based on Acoustic Emission Technique and Finite Element Analysis*. In: *Applied Surface Science* **255** (2008) Issue 5, Part 2, p. 3267-3275.
  13. Wang, D., Liang, E., Chao, M., Yuan, B.: *Investigation on the Microstructure and Cracking Susceptibility of Laser-Clad V<sub>2</sub>O<sub>5</sub>/NiCrBSiC Alloy Coatings*. In: *Surface and Coatings Technology* **202** (2008) Issue 8, p. 1371-1378.
  14. Zhang, S.H., Li, M.X., Cho, T.Y., Yoon: *Laser Clad Ni-Base Alloy Added Nano- and Micron-Size CeO<sub>2</sub> Composites*. In: *Optics & Laser Technology* **40** (2008), p. 716-722.
  15. Zhang, P., Liu, Z.: *Physical-Mechanical and Electrochemical Corrosion behaviors of Additively Manufactured Cr-Ni-Based Stainless Steel Formed by Laser Cladding*. In: *Materials & Design* **100** (2016), p. 254-262.